Study of a new concept of photovoltaic-thermal hybrid collector

Y.B. Assoa, C. Menezo and R. Yezou
Thermal Center of Lyon (CETHIL), Lyon, France

G. Fraisse
Laboratory of Optimization of the Design and Engineering of the Environment (LOCIE), University of Savoy, France

T. Lefebvre
SUNLAND21 Company, France

ABSTRACT

This work presents the first step of the development of a new concept of photovoltaic/thermal collector that will be combined with preheating air and/or water production. It consists in a simplified mathematical modeling of a PV/T air collector. The studied prototype is a component of metal sheet type which has an air gap at the backside and which can be integrated in roofs or in facades. The first step presented here consists in a parametric study (experimentally and numerically) in order to determine the effect of some factors as the air circulation (natural or forced) on the system thermal performances. Steady-state and a bi-dimensional geometry are considered. Then, an experimental confrontation led on a test bench permits to validate the results of the simulation and allows envisaging further development.

1. INTRODUCTION

Hybrid PV/T collectors produce electricity and heat (air or water preheating). The advantage is to ameliorate the global energy efficiency of PV(/T) modules by extracting the heat loose by using a heat removal fluid (air or water). Many theoretical and experimental studies have been made on hybrid air PV/T collectors.

Most of the thermal models proposed are based on a nodal approach.

Thus, Mei (2003), in the analysis of a ventilated PV air collector, determined the Nusselt number corresponding to the heat transfer coefficient for forced convection by taking into account the combination of a laminar and a turbulent flow of the fluid.

Guiavarch (2003) proposed a modeling of a PV hybrid air collector, which can be integrated in roofs.

Hollick (1999) reported the experimental study of a solar collector composed of metal perforated and corrugated sheet steel on which a solar panel is stuck.

Then, Belusko (2004) proposed the analysis of a solar air collector with a metal corrugated plate by comparing it to an unglazed solar collector. In our paper, a 2D simplified thermal model of a photovoltaic air collector is introduced. The final main function of this component will still remain production of electricity using solar energy. However, a first parametric study permits to evaluate the effect of many factors on the further thermal performances of this component especially for building air preheating configuration. Then, the results of simulation are compared to the experimental values obtained on a test bench led in controlled limit conditions.

2. COMPONENT THERMAL ANALYSIS

The photovoltaic air collector studied is shown schematically in Figure 1. It consists of a ribbed sheet steel absorber on which is fixed a PV plate through a fin adhesive layer of Tedlar. There is an air gap between the absorber and an insulation layer.

The prototype is investigated in two steps. First, a simplified 2D model of a non ventilated PV collector is developed. Then, the case of a ventilated air gap is considered. The models are based on a nodal approach according to some

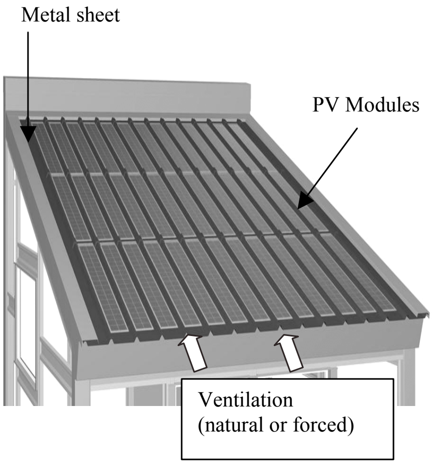

Figure 1: Scheme of the prototype of PV air collector.

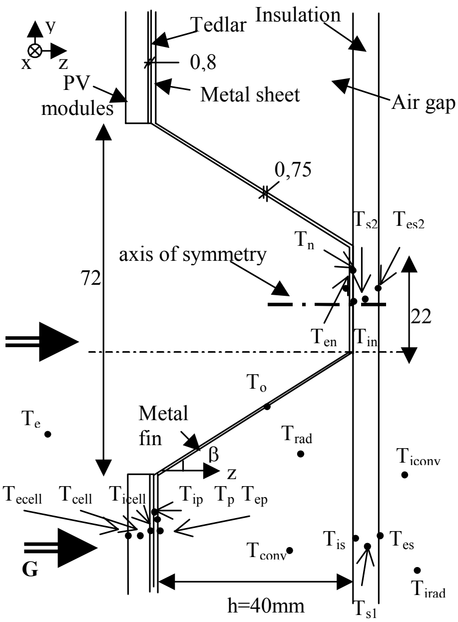

Figure 2: Cross section of the PV air collector and state variables.

assumptions.

The inclined part of the rib is compared to a fin bathing in two different fluids at constant temperatures.

The direct solar radiation G (W/m²) is supposed to be perpendicular to the collector surface.

By symmetry, only half of the rib and the solar panel is taking into account in the study.

2.1 Thermal model of the non ventilated PV air collector

The various layers constituting the system are represented by two or three nodes (Fig. 2). The node T_c represents the sky temperature, T_e represents the ambient air temperature, T_{ecell}, T_{cell} and T_{icell} are for the PV modules temperature, T_{en}, T_n and T_{in} are for the base of the rib, T_{ep}, T_p and T_{ip} are for the metal sheet,

T_{es}, T_{s1}, T_{is}, T_{s2} and T_{es2} are for the polystyrene insulation, T_{conv}, T_{rad} and T_f, are for the air gap and T_{iconv} and T_{irad} are for the temperature of the internal air of the building.

2.1.1 The inclined part of the rib

The energy conservation equation over the inclined part of the rib is considered as a classical fin case (Ammari, 2003). The node T_o is taken as the average temperature of this inclined wall. The radiation energy Q_o absorbed by this node is given by:

$$Q_o = G*\alpha_o*((b_1-b_o)/2)*L \qquad (1)$$

where:

- b_o: width of the base of the rib, in meter
- b_1: width of opening of the rib, in meter
- L: length of the collector, in meter
- α_o: absorptance of steel (-)

This fin effect calculation permits us to obtain the temperature T(z) function of the height z of the air gap and then at the node T_o located at
z =h/2 by writing the heat balance equation of the fin.

$$T(z) = (T_p-A/B)*\cos((\sqrt{B})*z)+(T_p-A/B) *(\sin((\sqrt{B})*h)/\cos((\sqrt{B})*h)) *\sin((\sqrt{B})*z)+A/B \qquad (2)$$

Where the parameters A and B are:

$$A = (h_{ce}*S_{e-o}*T_e+h_{conv}*S_{o-conv}*T_{conv} +h_{rad}*S_{o-rad}*T_{rad}+Q_o)/k_p*S_{o-p} \qquad (3)$$

$$B = (h_{ce}*S_{e-o}+h_{conv}*S_{o-conv} +h_{rad}*S_{o-rad})/k_p*S_{o-p} \qquad (4)$$

where:

k_i: thermal conductivity of the material i,

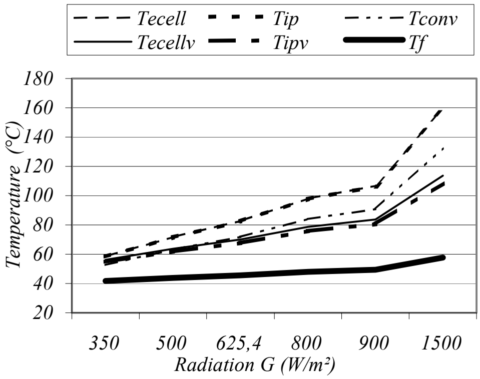

Figure 3: Temperatures of PV modules, of the absorber and of air according to solar radiation G in the case of a forced (v) and of a natural ventilation.

in W/m.K

h_i: heat transfer coefficient, in W/m².K

h: height of the air gap, in m

S_{i-j}: heat exchange surface between the nodes i and j, in m²

β: angle between the vertical and the inclined part of the rib, in degree.

A heat balance is written in every nodes according to the phenomena of coupled heat transfers. It is divided in two parts: the first part concerns the base of the rib and the second part concerns the air gap. The equations have the following form:

$\sum_i K_{i-j}*(T_i-T_j) = M_j*C_j*(dT_j/dt)$ for the central nodes,

or $\sum_I K_{i-j}*(T_i-T_j) = 0$ for the nodes of surface.

Where the conductance is written as:

$$K_{i-j} = h_{i-j}*S_{i-j} \quad (5)$$

2.1.2 Heat balance n° 1

The first heat balance includes the base of the rib and the insulation layer of polystyrene.

Since the tests have been carried out in a laboratory, we supposed that the local walls are at the ambient temperature T_e. Then, the sky temperature is considered equal to the laboratory ambient air ($T_c = T_e$) for radiation heat exchange equations.

$$0 = K_{rad,\,e-en}*(T_e-T_{en})+K_{n-en}*(T_n-T_{en})+K_{e-en}*(T_e-T_{en})+ G*\alpha_n*b_o*L/2 \quad (6)$$

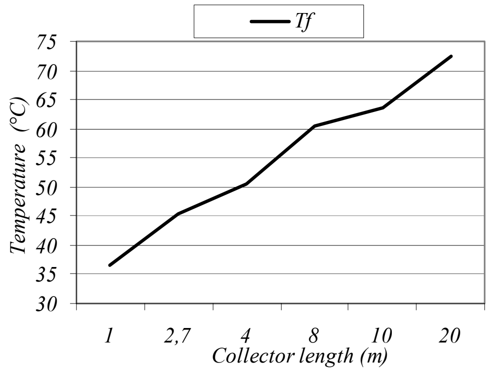

Figure 4: Temperature of air according to the collector length for T_{fin} = 29,4 °C.

Where:

$K_{rad,e-en}$: conductance for a radiation transfer between the nodes e and en, in W/K

$$M_n*C_n*(dT_n/dt) = K_{in-n}*(T_{in}-T_n) +K_{en-n}*(T_{en}-T_n) \quad (7)$$

where:

M_i: mass of the material i, in kg.

C_i: specific heat in J / kg K.

2.1.3 Heat balance n°2

The heat balance includes the insulation layer located under the air gap, the non ventilated air gap, the metal absorber and the photovoltaic cells.

$$M_{s1}*C_{s1}*(dT_{s1}/dt) = K_{s1-es}*(T_{es}-T_{s1}) +K_{s1-is}*(T_{is}-T_{s1}) \quad (8)$$

For the non ventilated air gap, the temperature T_{rad} is defined as the mean radiant tempera-

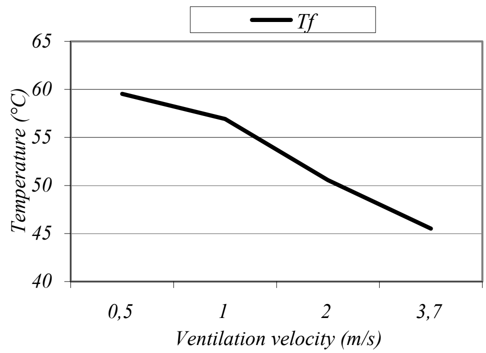

Figure 5: Temperature of air according to the velocity of air circulation.

ture of the walls of the gap.

$$0 = K_{ep\text{-}rad} * (T_{ep} - T_{rad}) + K_{o\text{-}rad} * (T_o - T_{rad}) + K_{is\text{-}rad}(T_{is} - T_{rad}) \quad (9)$$

$$M_{air} * C_{air} * (dT_{conv}/dt) = K_{ep\text{-}conv} * (T_{ep} - T_{conv}) + K_{o\text{-}conv} * (T_o - T_{conv}) + K_{is\text{-}conv} * (T_{is} - T_{conv}) \quad (10)$$

The convective heat transfer coefficient can be obtained from the Nusselt number for fully developed laminar flow in natural convection in ducts (Ammary, 2003): Nu = 4,36.

$$M_p * C_p * (dT_p/dt) = K_{ip\text{-}p} * (T_{ip} - T_p) + K_{ep\text{-}p} * (T_{ep} - T_p) + K_{o\text{-}p} * (T_o - T_p) \quad (11)$$

$$0 = K_{cell\text{-}ecell} * (T_{cell} - T_{ecell}) + K_{e\text{-}ecell} * (T_e - T_{ecell}) + K_{rad,e\text{-}ecell} * (T_e - T_{ecell}) + Q_{cell} \quad (12)$$

The radiation energy absorbed by photovoltaic cells takes into account electric conversion and is given by:

$$Q_{cell} = G * b_{cell} * (L/2) * \alpha_{cell} - E_p \quad (13)$$

where:

b_{cell}: width of the solar panel, in meter.

If r_c is the ratio of cells area to aperture area and η_{cell} is the temperature-dependent solar cell operating efficiency, the generated DC power E_p is given by:

$$E_p = G * b_{cell} * (L/2) * r_c * \eta_{cell} \quad (14)$$

The convective heat exchange coefficient between the cells surface and the ambient air can be obtained by the formula (Ammari, 2003):

$$h_{e\text{-}ecell} = 3{,}8 * u_e + 5{,}7 \quad (15)$$

where:

u_e: the ambient air velocity (m/s).

2.2 Modeling of the ventilated PV air collector

In the case of a ventilated air gap, the air is represented by the node T_f. The equations in the heat balance change only with certain nodes. Concerning the node T_o, the result is similar to equation (6) but $T_{f\ \text{replaces}\ T_{conv}}$ in the formulas of the parameters A and B

The ventilated air gap is represented by node T_f.

$$q_m * C_p * (T_f - T_{fin}) + M_f * C_f * (dT_f/dt) = K_{f\text{-}is} * (T_f - T_{is}) + K_{ep\text{-}f} * (T_{ep} - T_f) + K_{o\text{-}f} * (T_o - T_f) \quad (16)$$

where:

q_m: mass flow rate of air in kg/s
C_p: specific heat of air in J/kg.K

The Nusselt number Nu for forced convection in the ventilated gap can be obtained from Petukhov equation (1970) for fully developed turbulent flow in tubes or ducts.

$$Nu = [(f/8) * Re * Pr]/[1{,}07 + 12{,}7 * \sqrt{((f/8) * (Pr^{2/3} - 1))}] * (\mu/\mu_w)^{0{,}11} \quad (17)$$

where:

Re: Reynolds number
Pr: Prandtl number
μ_w: dynamic viscosity of water, in kg/m.s
f: is a friction factor given by:

$$f = (0{,}79 * \ln(Re) - 1{,}64)^{-2} \quad (18)$$

3. EXPERIMENTAL COMPARISON

An experimental study on the prototype described was led by the Sunland21 Company on a test bench and permits to obtain experimental values of temperature in various preset points of the collector for two types of configurations. The tests were carried out in steady state and in controlled radiation conditions.

3.1 Description of the experimental device

The sheet steel was placed in a box of dimensions 2,7 m x 0,6 ml x 0,45 m (Photo 1). The slope of the box is adjustable from 0° to 15°.

The internal walls of the box are covered with 5 mm of polystyrene. Three directional gas-discharge lamps offering a maximum power of 1500 W/m² ensure the radiation. The inten-

Photo 1: Photograph of the test bench gone up by the Sunland21 Company.

Table 1: Comparison of simulation results and experimental results.

	Tcalculated	Texp right	Texp left
Tecell	82,7	80	85,7
Ticell	82,6		
Tip	82,5		
Tep	82,4	82,4	86,7
Tconv	71,8		
T(h/2)=To	82,6	80,9	81
Ten	82,7	79,2	79,2

sity of radiation was measured using a flux-meter. The air velocity at the entry of the gap is adjustable with a ventilator from 0 to 5 m/s. For the air velocity measurement, probes speeds were used.

3.2 Analysis of simulation results

3.2.1 Non ventilated PV air collector

The tests realized provided the following results for a radiation G =625 W/m² (Table 1).

3.2.2 Ventilated PV air collector

The tests carried out provided the following results for a radiation G =625 W/m² and a mean velocity of ventilation of V=3,7 m/s. The inlet air temperature is of 29,4 °C (Table 2).

After comparison, the values obtained during the simulation are very close to the experimental values. The differences can be explained in particular by the fact that during calculations, the radiation was supposed uniformly distributed on all the surface of the collector, which was not checked during the tests carried out by the Sunland21 Company.

4. PARAMETRIC STUDY

A study was undertaken on the collector for the two types of configurations in order to evaluate the influence of parameters such as the solar radiation G, the length of the gap L and the velocity of air circulation V in the gap on its thermal performances.

Table 2: Comparison of simulation results and experimental results

	Tcalculated	Texp left	Texp right
Tecell	70,0	69,2	72,8
Ticell	69,8		
Tip	67,7		
Tep	67,7	67,7	69,2
Tf	45,5	46	48
T(h/2)=To	67,8	66,7	63,7
Ten	67,9	66,7	

4.1 Effect of solar radiation G

A parametric study was carried out in order to determine the influence of the radiation G on the temperature of the air at the exit of the gap, on that of the upper surface of the PV modules and on that of the back face of the absorber for a natural ventilation simulation (T_{conv}, T_{ecell} and T_{ip}) and for a forced ventilation simulation (T_f, T_{ecellv} and T_{ipv})

The value of radiation varies from 350 W/m² to 1500 W/m². The air velocity in the ventilated solar collector is fixed at 3,7 m/s.

The analysis of the graphs obtained shows that the absorber and the PV cells curves are confused, so we can said that a good ventilation of the steel absorber is enough with cooling to PV modules.

4.2 Influence of the length of the gap on the fluid temperature

A parametric study was carried out on the fluid temperature at the exit of the gap while varying the length of the ventilated PV air collector.
The fluid temperature is doubled approximately when the length of the collector goes from 1 to 20 m.

4.3 Influence of air circulation velocity on the fluid temperature

A study was carried out on the air temperature at the exit of the collector while varying the air velocity.

The analysis of the curve shows that the air temperature decreases when the air circulation velocity increases.

Compared to the variation of the collector length, the reduction in mass flow rate seems the most practical solution to increase the collector efficiency because it doesn’t need to modify its dimensions.

5. CONCLUSION

A mathematical model of the PV air collector presented was proposed according to whether the ventilation of the air gap is natural or forced. Then, an experimental study confirmed the values obtained during simulation. A parametric study carried out permitted to find the awaited tendencies concerning the temperature of cells and of the fluid at the outlet side of the air gap according to the velocity of ventilation, the collector length and the received radiation. We note that forced ventilation is obviously the best (in particular in summer) for the thermal efficiency of the collector. It would be also interesting to examine if natural ventilation can sufficiently support in real conditions a production of an optimal quantity of electricity.

Thus, we will develop the model by integrating an electric balance. Currently, we instrument this collector in a phase of building integration (Fig. 1) within the framework of a project ADEME PUCA titled "Building at Horizon 2000" carried out in partnership with Sunland21, ARCELOR, TOTAL Energy companies and the CSTB (Building Scientific and Technical Center) laboratory. In the second part of this work, an evolution permitting to integrate a function of production of hot water will be proposed.

REFERENCES

Ammari, H.D. (2003). A mathematical model of thermal performance of solar air heating with slats. Renewable Energy, Karak, vol.28: pp.1597-1615.

Belusko, M. (2004). Roof integrated solar heating system with glazed collector ventilated PV façade. Thèse Energétique-Environnement, Mawson Lakes, vol.76: pp.61-69.

Guiavarch, A. (2003). Etude de l'amélioration de la qualité environnementale du bâtiment par intégration de composants solaires, Université de Pontoise, Cergy-Pontoise, 311p..

Hollick, J.C. (1998). Solar cogeneration panels, Renewable Energy, Toronto, vol.15: pp.195-200.

Mei, L. (2003). Thermal modeling of a building with an integrated ventilated PV façade, Energy and buildings, Stuttgart, vol.35: pp.605-617.

Petukhov, B.S. (Hartnett JP, Irvine TF New York: Academic Press) (1970). Heat transfer and friction in turbulent pipe flow with variable physical properties, Advances in heat transfer, New York, p. 504-64.